Transparent Electrostatic Actuator with Mesh-structured Electrodes for Driving Tangible Icon in Tabletop Interface

Ryuta Iguchi, Takuya Hosobata and Akio Yamamoto
Department of Precision Engineering, School of Engineering
The University of Tokyo
Tokyo, Japan.
{r.iguchi, hosobata, akio}@aml.t.u-tokyo.ac.jp

***Abstract*—This paper proposes a transparent electrostatic actuator for actuating tangible objects in a tabletop interface. The actuator is a planar actuator with two degrees-of-freedom, capable of actuating a small dielectric sheet placed on top. The feature of the actuator is in having mesh-structured electrodes, patterned on a transparent film using a conductive polymer. By applying pulse voltages to the electrodes, electrostatic force act on the charges induced on the sheet to produce step-wise motion. The transparency of the actuator enables this actuation while maintaining the visibility of graphics on a visual display underneath. To demonstrate the suitability of the actuator for a tabletop interface, we constructed a simple human-computer interaction system, in which a physical icon travels on the actuator placed on a flat panel display. In the demonstration, the user could interact with the computer by handling active and passive tangible icons. The actuator used in the system could actuate a small icon in a broad area of 300 mm by 300 mm, with application of 500 V pulse voltages.**

Keywords-tangible media; tabletop interface; human-computer interaction; surface actuator; electrostatic actuator.

I. INTRODUCTION

In 1997, Ullmer and Ishii showed that great enrichment is brought to a tabletop interface by bringing in physical objects as tangible media to coexist with a visual display [1]. A way to further improve such an interface was demonstrated by Pangaro et al., which is to have the tangible objects actuated [2]. Actuated tangibles let the computer inform us of its internal state through their physical motion, which we can comprehend with familiarity. In this paper, we introduce an actuator developed for such tabletop interface: a transparent electrostatic actuator with mesh-structured electrodes. In addition, we prove its effectiveness through a simple tabletop interaction, which is illustrated in Fig. 1. The actuator specializes in actuating physical icons on a surface of a Flat Panel Display (FPD).

Forms and functions of active tangibles vary depending on types of interactions expected in the tabletop interface. To satisfy the requirements of each case, it is important to choose the proper means of actuation. To have the active tangibles represent handheld-sized objects, the most effective way is to have the objects move by themselves, that is, to use wheeled robots [3][4] or legged robots [5]. An advantage of this solution is that multiple robots can collaborate to perform various tasks. However, shapes and sizes of the objects representable with robots are limited by their functionality; the robots must carry batteries and driver electronics, which prevents the robots to disguise as physical icons that do not resemble them.

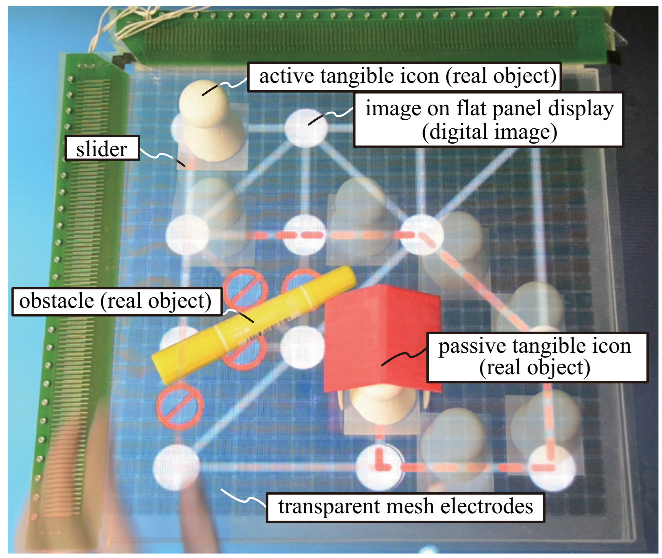

Figure 1: Conceptual photograph of tabletop interface on flat panel display with tangible icon actuated by mesh-structured electrostatic actuator.

To have physical icons of various shapes actuated, a tabletop interface must incorporate an actuator capable of driving objects on a displayed image. Various magnetic surface actuators satisfy this requirement, which include electromagnet arrays [2][6], planar induction motors [7] and sawyer motors [8]. Magnetic levitators are also effective, providing an actuation in mid-air [9][10][11]. These actuators have excellent driving performance, but the drawback is in requiring ferromagnetic cores embedded in the system, which consume space and increase the total weight of the system.

As another choice of actuator for actuating physical icons, we propose a transparent electrostatic actuator, which we can easily install on an FPD. The original concept of the transparent actuator was proposed by Egawa et al. in 1991 [12]. The actuator is a transparent plastic film with array of strip-electrodes made of transparent conductors. The film drives dielectric sheets (e.g., papers, plastics, and glass) placed on its surface, by electrostatic forces excited by voltages applied

 ISBN: 978-1-61208-325-4

to the electrodes. The actuator is suited for tabletop interface because of its transparency and thinness; simply by placing it on top of a visual display, we can drive objects while maintaining visibility of displayed images.

Previously, we reported an FPD-based interaction using the transparent electrostatic actuator, in which users could play catch with an animated cat, using a ball printed on a paper sheet [13]. In this system, the actuator could actuate the ball only in one direction. To realize multi-directional motion, we developed a transparent actuator with 2-DOF [14], and demonstrated a mixed-reality on an FPD, in which an animated robot could interact with a small ball driven based on virtual dynamics [15]. One problem of this actuator was in having short stroke; it could move the ball only within a small area of the FPD, because the actuated film was much larger with respect to the ball it carried. Such restriction in stroke was caused by the actuator's electrode structure. Thus, as a next step, we chose to develop a 2-DOF transparent actuator that can actuate small films in a broad area.

The transparent electrostatic actuator we developed in this work has mesh-structured electrodes, which realize actuation of small objects with large stroke. The idea of using mesh as electrodes in an electrostatic actuator is already reported using woven copper wires [16]. We combined this idea with the concept of transparent actuator, and developed an actuator with *printed* mesh, fabricated by screenprinting using a transparent conductive polymer. In the mesh, there are vertical and horizontal *printed* belts, containing three-phase electrodes. The belts intersect in a manner that electrodes producing different directioned forces appear on the surface alternately. When the electrodes are excited with pulse voltages, electrostatic forces arise to give a step-wise motion to a dielectric sheet placed on top. We designed the belts to be 12 mm in width, which makes the minimum size of the driven film twice this size. The actuator itself has an area of 300 mm by 300 mm, which allows long distance travel of the actuated sheet. With the long stroke and the transparency, the actuator enables planar actuation on visual displays, which is especially useful for tabletop interfaces.

The rest of the paper is organized as follows. In Section II, we explain the structure and driving principle of the transparent actuator. Then, we report on the evaluation of the actuator's performance in Section III. Finally, in Section IV, we demonstrate the actuator's suitability for tabletop interfaces through a simple human-computer interaction with a physical icon driven on an FPD.

II. Transparent Electrostatic Actuator with Mesh Electrodes

This section provides explanations on the structure and the driving principle of the transparent mesh actuator shown in Fig. 2. Details on the principle of 1-DOF actuator is reported in [12]; the same principle applies to this actuator, but with an extra DOF.

A. Structure of the Actuator

Fig. 3 shows the basic structure of the actuator. The actuator consists of two films; we refer to the fixed film as the stator and the driven film as the slider. The stator has a polyethylene terephthalate (PET) film with 100 μm thickness as a substrate. On the surface of this film, patterns of electrodes and insulators are printed by screenprinting technology. The electrodes are strips of transparent conductive polymer: poly(3,4-ethylenedioxythiophene):poly(4-styrenesulfonate) (PEDOT:PSS), 400 μm in widths and spaces, printed in two layers. We chose this polymer because of its transparency and compatibility with the screenprinting; the polymer appears in pale blue, but is transparent enough to see through the actuator.

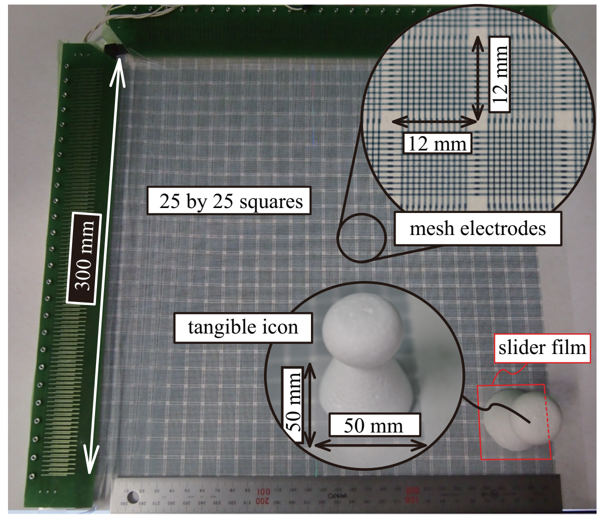

Figure 2: Photograph of the transparent electrostatic actuator with mesh electrodes.

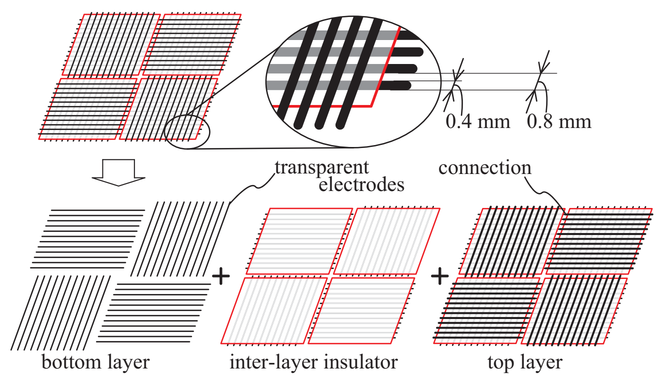

Figure 3: Structure of the transparent electrostatic actuator with mesh electrodes.

The electrodes in the bottom layer are directly printed on the PET film. There are vertical electrodes and horizontal electrodes; the former are the X electrodes and the latter are the Y electrodes, which respectively drive the slider in directions X and Y. The X and Y electrodes are separated in small squares, arranged alternately as in a checkerboard pattern. Note that in this layer, electrodes in all squares are isolated from each other. Lengths of the sides of each square are 12 mm, and each contains twelve electrodes. There are 25 by 25 squares in total, which makes the total length of the stator 300 mm.

On top of the bottom-layer electrodes, there is a inter-layer insulator, which is also screenprinted using thermo-setting polymer paste. The insulator covers most of the bottom-layer electrodes, but leaves the ends of the electrodes uncovered.

Over this inter-layer insulator, top-layer electrodes are printed. These electrodes are arranged in different directions from the bottom-layer electrodes; X electrodes are printed over Y electrodes and vice versa. The top-layer electrodes are connected at their ends to the bottom-layer electrodes, in areas not covered by the inter-layer insulator. Thus, the connected X and Y electrodes form 300 mm long belts, which appear as if they are woven, with X and Y belts alternately appearing to the surface. Finally, the surface is covered with another insulating layer, on which the slider is driven.

The stator is very thin; each of the insulating layers are approximately 20 μm thick, which makes the total thickness of the stator 147 μm. Thickness of the electrodes are 2 μm, almost negligible compared to the film thickness. The thinness, together with the transparency, provides a feeling that the slider is driven directly on the images displayed underneath.

As a slider, we could choose from various dielectric sheets, such as paper, plastic or glass. In this work, we chose to use a slider with PET sheet 50 mm $\times$ 50 mm as a substrate, with its top surface coated with glass particles 100 μm in diameter. This slider was chosen empirically; the slider performed the best among those we tested. There is an interesting problem in the optimization of materials for the slider, which we leave for future works.

B. Driving Principle

Fig. 4 shows the patterns of voltages applied to the electrodes to drive the slider in different directions. The X and Y electrodes in the outer most squares are connected to three-phase buses, to which three-phase pulse voltages are applied. The slider is driven in the X direction by shifting the pulse voltages on X electrodes while the electrodes of Y are grounded, and the similar applies to driving in the Y direction. To drive the slider in a diagonal direction, we shift pulses on both X and Y electrodes.

Fig. 5 schematically illustrates the induced charges on the slider and the electrostatic forces acting on them. The driving sequence consists of three steps: charging, shifting and stepping. First in charging, the electrostatic field excited by the applied voltages induce charges of corresponding polarity on the slider. Then the voltage pattern is shifted in the driving direction, but the arrangement of charges lags behind because the slider has a low conductivity. Finally, electrostatic forces act on the lagged charges and steps the slider forward.

For the slider used in this work, 10 to 30 seconds of pre-charging was necessary as a preparation for driving. This is because the time constant for the charges to arise or decay was on the order of seconds. Once the slider was pre-charged, constant shifting of voltages could drive the slider full-stroke in one direction. However, occasional re-charging was necessary when the slider had to turn 90 degrees. For example, without this re-charging, the slider could not move in Y direction after traveling full-stroke in X direction. The reason is still unclear, but we presume that the charges required for driving in Y direction diminish while the slider is traveling in X direction.

The stepping distance of the slider depends on the balance

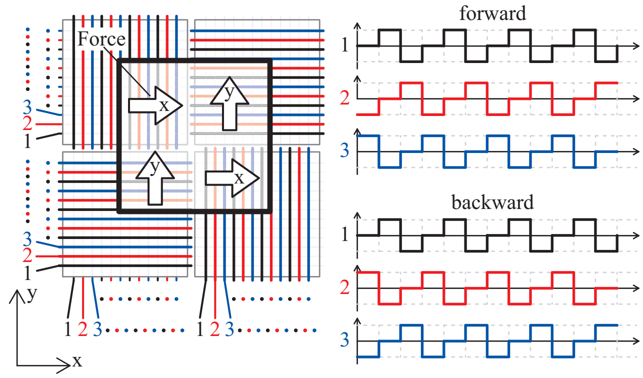

Figure 4: Voltage patterns applied to the electrodes in the mesh actuator.

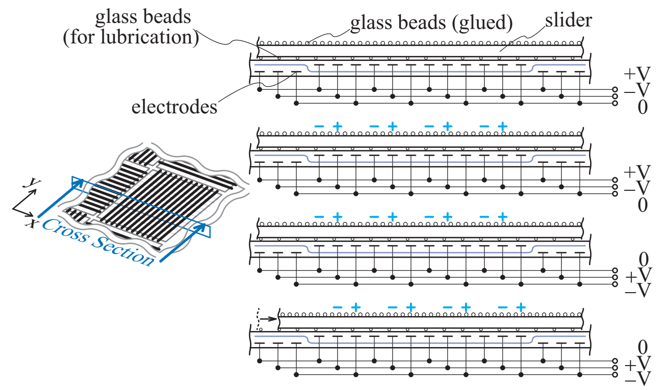

Figure 5: Schematic of driving principle of the mesh actuator.

of thrust and frictional force. With the actuator of this work, the friction is small enough and the stepping distance per pulse is nearly equal to the length of an electrode pitch: 800 μm. This characteristic allows us to roughly control the position of the slider in open-loop. In the application in Section IV, we take advantage of the characteristic to realize variety of motions with a simple control method.

III. Performance Evaluation

We conducted two experiments to evaluate the actuator's performance. First, we tested for the maximum speed the slider could travel. Then, we confirmed the actuator's capability of actuating the slider over all areas of the stator in different directions.

sends it to a DSP (DS1104, dSpace [17]) in Fig. 2, which is made of a polystyrene foam and weighs 0.48 grams. The magnitude of the pulse voltage was fixed at $\pm$500 V and glass beads of 20 μm diameter were scattered on the surface of the stator to reduce friction. Before each experiment, the slider was pre-charged by applying $(500,\ -500,\ 0)$ V DC voltages to both of X and Y electrodes for 30 seconds.

A. Maximum Speed

We drove the slider in X direction with pulse voltages of different frequencies, to see how fast the slider can travel while carrying the icon. Fig. 6 shows the motion of the slider driven

 ISBN: 978-1-61208-325-4

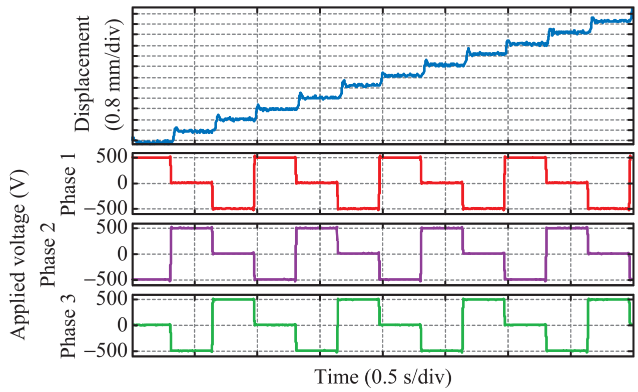

Figure 6: Step-wise motion of slider carrying icon and applied three-phase pulse voltage.

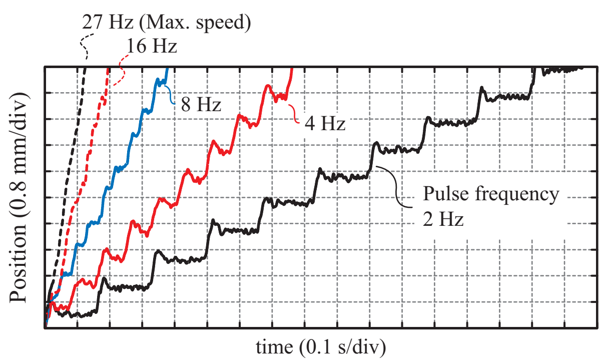

Figure 7: Motion of the slider driven by 500 V three-phase pulse voltages with different frequencies.

by 1 Hz pulse voltage in X direction, recorded using laser displacement sensor (Keyence LB-01). This result shows that the slider travels 2.4 mm per one cycle of the three-phase pulse, which is equal to the length of three electrode pitches. Fig. 7 shows the results with higher frequencies. The results indicate that the step-wise motion is damped as the speed increases with the frequency. This is because the inertia of the slider and the friction disable the slider to instantly respond to the pulsating force.

When the frequency exceeded 27 Hz, the slider stood still at its initial position; the maximum speed was approximately 64 mm/s. The speed is nearly equal to the frequency times three electrode pitches ($27\ \mathrm{Hz} \times 2.4\ \mathrm{mm} = 64.8\ \mathrm{mm/s}$). This indicates that even at the maximum speed, the traveling distance of the slider is controllable by the number of voltage pulses. Thus, we can assume that the position of the slider is roughly controllable in open-loop.

B. Full-stroke motion

To confirm the actuator's capability as a long-stroke surface actuator, we recorded the full-stroke motion of the slider in different directions. In this experiment, the frequency of the pulse voltage was fixed at 5 Hz, and trajectories of the slider were recorded using a visual motion tracking system with high-speed camera (VW-6000, Keyence). The results are shown in Fig. 8, indicating that slider was successfully driven over the

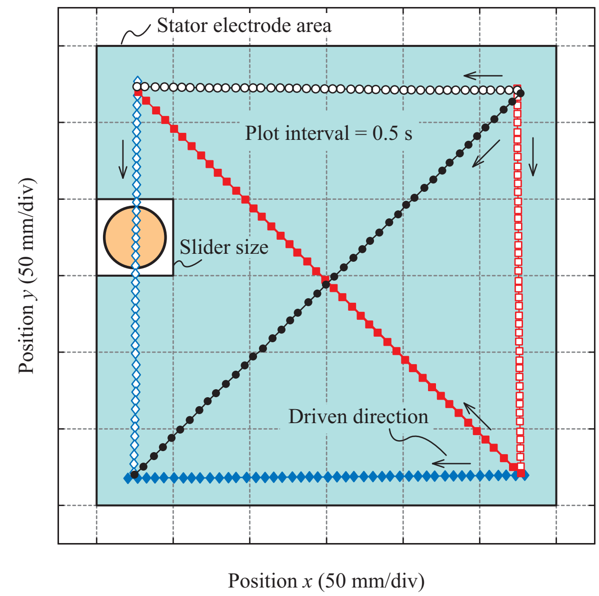

Figure 8: Result of Motion Tracking.

whole 300 mm × 300 mm area of the stator.

We expect that driving in intermediate angles (such as 30 degrees) is possible in principle, by exciting X and Y electrodes with pulse voltages of different frequencies. However, we could not realize such motion in this work; cause of this is still under investigation.

IV. Tangible Interaction Using Mesh Actuator

To demonstrate the actuator's suitability for tabletop interfaces, we constructed a simple interaction system illustrated in Fig. 9. In this system, the transparent mesh actuator covers an FPD, which is displaying an undirected graph. The actuator drives the person icon carried by the slider along the shortest path leading to another icon, which represents the person's home.

The user of this system can take three actions to interact with the computer. First, the user can pick up and move the person icon. Second, the user can move the home icon to change the destination of the path. In addition, the user can block the path by placing an obstacle (a marker pen). All these actions are monitored by the computer, as it is constantly tracking the positions of the objects using a web camera(PlayStation Eye, Sony Computer Entertainment). The computer responds to the actions by rerouting the path, and the result is presented to the user not only by the displayed images, but also by the person icon's actual motion.

A. Control Approach

Fig. 10 shows how the person icon is controlled during the interaction. The person icon and the home icon have their own nodes aside from those in the preset graph, and these nodes are automatically connected to nearby links.

The computer constantly updates the shortest path from the person icon to the home icon using the Dijkstra's al-

 ISBN: 978-1-61208-325-4

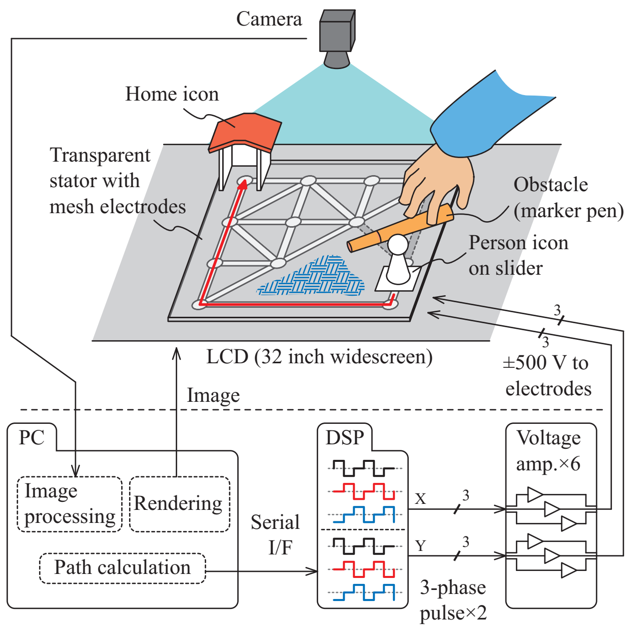

Figure 9: Configuration of the tangible tabletop interface using transparent mesh electrostatic actuator.

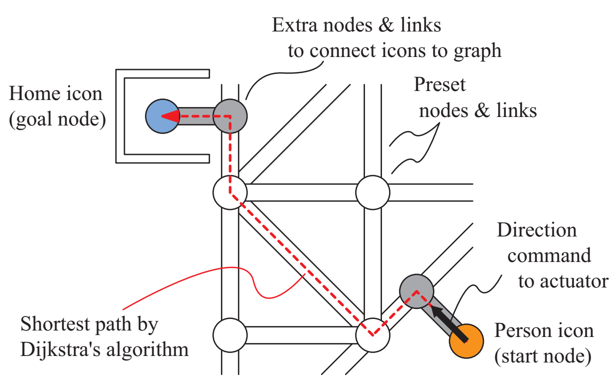

Figure 10: Control approach to drive the slider along the shortest path.

gorithm. Based on the calculated path, the computer detects the direction from the person icon to the next node in the path, and sends it to a DSP (DS1104, dSpace [17]). The DSP generates waveforms of three-phase pulses corresponding to the direction. The pulses are amplified by High-Voltage Amplifiers (HVA4321, NF Co. [18]) and applied to the electrodes to drive the person icon in the specified direction.

An exceptional condition is when the person icon is too close to the next node. In such a condition, the computer uses the direction from the person icon to the node after the next. This exceptional procedure was necessary, because without it the person icon would stop advancing and start oscillating around the next node. In this work, we applied the procedure when the icon was within a 10 mm diameter circle of the next node.

We chose this simple control approach because the mesh actuator can generate step-wise motion. This motion ensures that the driven icon does not overshoot beyond the next node by long distance. With this characteristic, specifying direction was sufficient to keep the driven icon on the planned path. Such simplicity in control is one advantage of this actuator, especially for tabletop interfaces using visual tracking; realizing fast servo control is difficult with cameras, whose frame rate limits the speed of the control cycle.

B. *Motion of the Slider During Interaction*

Fig. 11 shows the motion of the person icon recorded by tracking camera during three interaction experiments. In these experiments, the computer responded to the three actions from the user by rerouting the driven path of the person icon. In each experiment, the slider film carrying the person icon was pre-charged for 30 seconds by applying $(500, -500, 0)$ V DC voltages to both X and Y electrodes, and then driven at 7.2 mm/s by a ± 500 V three-phase pulse voltage. As explained in Section II-B, the slider film was re-charged for 10 seconds every time it had to make a 90 degrees turn. The re-charging was done by applying the same set of voltages as in pre-charging.

Fig. 11a shows the result of the user repositioning the person icon. At first, the person icon was traveling from the upper-right corner toward the home icon, along the shortest path in the graph. Then, the user picked the person icon up and repositioned it to prompt the computer to reroute the path, along which the person icon continued its travel. Fig. 11b and Fig. 11c show the result of the user's indirect action of handling passive tangible objects. In Fig. 11b, the user extended the travel of the person icon by changing the position of the home icon, which is the destination of the path. Fig. 11c shows the result of placing a marker pen: the obstacle, to block the preplanned path. The computer immediately detected that the links in the preplanned path is no longer available and rerouted the path.

C. *Problems*

The results prove that the proposed actuator realizes a variety of human-computer interaction by allowing active (driven) and passive tangible objects to collaborate with computer graphics on a surface of an FPD. However, through these experiments, we also found some problems of the actuator.

First, the charging time needs to be shortened, because the waiting time during the charging prevents the user from being immersed in the interaction. Second, the gripping force of the slider need to be increased. The user could touch and feel the person icon, but was provided with no force feedback, because of the low friction, light weight and weak force. These problems indicate that further improvements are necessary in terms of materials, design and driving method of the actuator.

V. Conclusion and Future Works

In this paper, we proposed a transparent electrostatic actuator with mesh-structured electrodes especially designed for tabletop interaction. With a working prototype, we proved the actuator's capability of presenting various planar motions of a physical icon together with graphics displayed on an FPD underneath the actuator. To extend the actuator's application

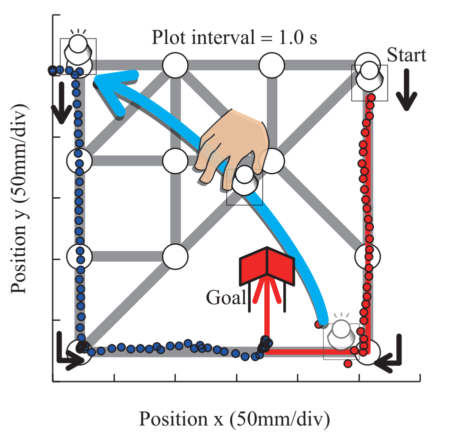

(a) Repositioning active icon (person icon).

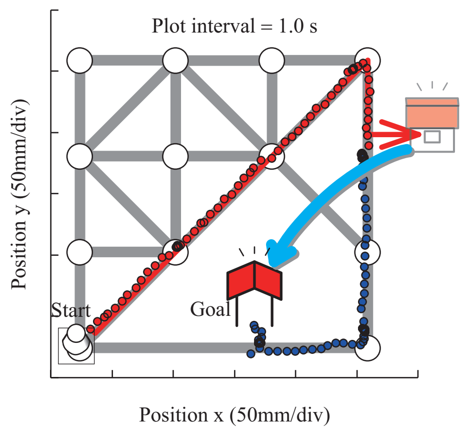

(b) Changing destination by moving passive icon (home icon).

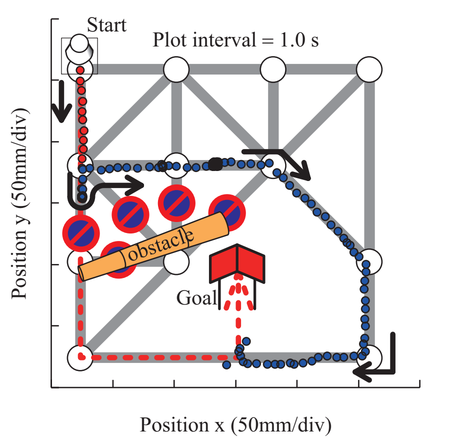

(c) Path blocking by placing obstacle (marker pen).

Figure 11: Rerouted path of person icon by user's handling of tangible icons. Plots indicate trajectory of person icon recorded with tracking camera.

range, a challenge lies in simultaneous actuation of multiple objects. In future works, we expect to realize this by independently controlling the voltages on different sections of the actuator.

ACKNOWLEDGMENT

This work was supported by Funding Program for Next Generation World-Leading Researchers (#LR013) from JSPS, Japan.

REFERENCES

[1] B. Ullmer and H. Ishii, "The metaDESK: models and prototypes for tangible user interfaces," In Proc. of the 10th Annual ACM Symposium on User Interface Software and Technology, 1997, pp. 223–232.

[2] G. Pangaro, D. Maynes-Aminzade, and H. Ishii, "The actuated workbench: computer-controlled actuation in tabletop tangible interfaces," In Proc. of the 15th Annual ACM Symposium on User Interface Software and Technology, 2002, pp. 181–190.

[3] E. W. Pedersen and K. Hornbæk, "Tangible bots: interaction with active tangibles in tabletop interfaces," In Proc. of the 2011 Annual Conf. on Human Factors in Computing Systems, 2011, pp. 2975–2984.

[4] M. Sugimoto, T. Fujita, H. .Mi, and A. Krzywinski, "RoboTable2: a novel programming environment using physical robots on a tabletop platform," In Proc. of Int. Conf. on Advances in Computer Entertainment Technology, 2011, pp. 10:1–10:8.

[5] S. Somanath, E. Sharlin, and M. C. Sousa, "Integrating a robot in a tabletop reservoir engineering application," In Proc. of ACM/IEEE Int. Conf. on Human-robot Interaction, 2013, pp. 229–230.

[6] M. Weiss, F. Schwarz, S. Jakubowski, and J. Borchers, "Madgets: actuating widgets on interactive tabletops," In Proc. of the 23nd Annual ACM Symposium on User Interface Software and Technology, 2010, pp. 293–302.

[7] S. Yoshida, H. Noma, and K. Hosaka, "Proactive Desk II: Development of a New Multi-object Haptic Display Using a Linear Induction Motor," In IEEE Virtual Reality Conf., 2006, pp. 269–272.

[8] M. Sugi et al., "Motion Control of Self-Moving Trays for Human Supporting Production Cell "Attentive Workbench"," In Proc. of the IEEE International Conf. on Robotics and Automation, 2005, pp. 4080–4085.

[9] J. Lee, R. Post, and H. Ishii, "ZeroN: mid-air tangible interaction enabled by computer controlled magnetic levitation," In Proc. of ACM Symp. on User Interface Software and Technology, 2011, pp. 327–336.

[10] M. Marshall, T. Carter, J. Alexander, and S. Subramanian, "Ultra-tangibles: creating movable tangible objects on interactive tables," In: Proc. of SIGCHI Conf. on Human Factors in Computing Systems, 2012, pp. 2185–2188.

[11] P. Berkelman, M. Miyasaka, and J. Anderson, "Co-located 3D graphic and haptic display using electromagnetic levitation," In: Proc. of Haptics Symp., 2012, pp. 77–81.

[12] S. Egawa, T. Niino, and T. Higuchi, "Film actuators: Planar, electrostatic surface-drive actuators," In Proc. of the IEEE Micro Electro Mechanical Systems Workshop, 1991, pp. 9–14.

[13] K. Amano and A. Yamamoto, "Tangible interactions on a flat panel display using actuated paper sheets," In Proc. of the ACM Int. Conf. on Interactive Tabletops and Surfaces, 2012, pp. 351–354.

[14] T. Hosobata, A. Yamamoto, and T. Higuchi, "2-DOF Synchronous Electrostatic Actuator with Transparent Electrodes Arranged in Checkerboard Patterns," In Proc. of IEEE/RSJ Int. Conf. on Intelligent Robots and Systems, 2013, pp. 4919-4924.

[15] T. Hosobata and A. Yamamoto, "Mixed Reality System on Flat Panel Display with Real Object Driven by Synchronous Transparent Electrostatic Actuator," In Proc. of Int. Conf. on Multimedia and Human Computer Interaction, 2013, pp. 127:1–127:7.

[16] A. Yamamoto, H. Yoshioka, and T. Higuchi "A 2-DOF Electrostatic Sheet Conveyer Using Wire Mesh for Desktop Automation," In Proc. of IEEE Int. Conf. on Robotics and Automation , 2006, pp. 2208–13.

[17] http://www.dspace.com/en/pub/home/products/hw/singbord/ds1104.cfm Last accessed on 10/Feb/2014.

[18] http://www.nfcorp.co.jp/english/pro/pp/p_amp/h_vol/hva4321/index.html Last accessed on 10/Feb/2014.